Supplementary Information for:

A Robust Metal-Organic Framework for Post-Combustion Carbon Dioxide Capture

Omid T. Qazvini and Shane G. Telfer*

MacDiarmid Institute for Advanced Materials and Nanotechnology, School of Fundamental Sciences, Massey University, Palmerston North, New Zealand

Contents

1. Synthesis 2
2. Single crystal X-ray diffraction 3
3. Powder X-ray diffraction patterns 4
4. Thermogravimetric analysis 5
5. Gas adsorption measurements 6
6. Heat of adsorption 9
7. IAST calculations 10
8. Breakthrough separation experiment 15
9. Breakthrough curve simulation 18
   9.1. Mathematical modelling 18
   9.2. Numerical methods 20
10. Pelletization 22
11. References 22

1. Synthesis

MUF-17 was synthesized by a one-pot reflux reaction on both small and large scales. All starting reactants and solvents were obtained from commercial sources and used without further purification.

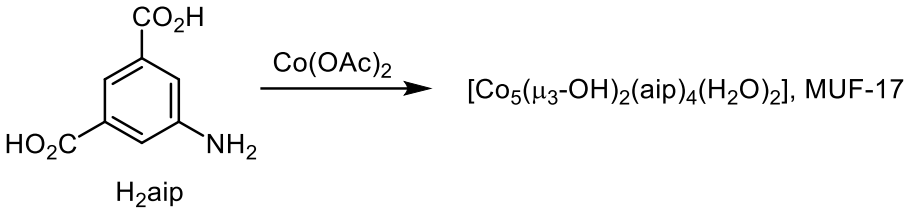

Small-scale synthesis:

A mixture of $Co(OAc)_2 \cdot 4H_2O$ (1.25 g, 5.0 mmol), 5-aminoisophthalic acid (H_2aip, 0.46 g, 2.5 mmol), MeOH (70 mL), and H_2O (5.0 mL) were mixed in a 200 mL round bottom flask by sonicating for 5 min. The mixture was then was then heated to reflux for 8 hours. After cooling, the resulting purple crystals were isolated by decanting off the mother liquor, then washed with methanol several times and dried under vacuum. Yield *ca.* 0.63 g, 93% (based on H_2aip). Guest-free MUF-17 could be obtained by heating under high vacuum at 130 °C for 20 h. This method yields larger and high quality crystals compared to the solvothermal synthesis procedure reported previously.[1]

Large-scale synthesis:

A mixture of $Co(OAc)_2 \cdot 4H_2O$ (18.75 g, 75 mmol), 5-aminoisophthalic acid (H_2aip, 6.9 g, 37.5 mmol), MeOH (800 mL), and H_2O (65 mL) were mixed in a 1 L round bottom flask by sonicating for 5 min. The mixture was then was then heated to reflux for 8 hours. After cooling, the resulting purple crystals were isolated by decanting off the mother liquor, then washed with methanol several times and dried under vacuum. Yield *ca.* 9.6 g, 94% (based on H_2aip).

While this was the largest scale synthesis that we attempted, we foresee no problems in extending this method to even greater quantities.

2. Single crystal X-ray diffraction

Given the larger dimensions and better crystal quality compared to our earlier synthetic method,[1] we have collected single crystal X-ray diffraction data. A Rigaku Spider diffractometer equipped with a MicroMax MM-007 rotating anode generator (Cu_α radiation, 1.54180 Å), high-flux Osmic multilayer mirror optics, and a curved image plate detector was used.

MOF crystals were analysed after removing them from methanol. Room temperature data collections produced better refinement statistics than low temperature data collections. All atoms were found in the electron density difference map. A mask was used to account for the porous regions of the framework with disordered solvent. All atoms were refined anisotropically, except the hydrogen atoms, which were placed in calculated positions and refined using a riding model.

Table S1. Crystal data and structure refinement for MUF-17.

CCDC deposition number	1996148
Formula	$Co_5(\mu_3\text{-}OH)_2(aip)_4(H_2O)_2.6H_2O$
Empirical formula	$C_{32}H_{38}Co_5N_4O_{26}$
Formula weight	1189.31
Temperature/K	293
Crystal system	monoclinic
Space group	C2/c
a/Å	35.22(3)
b/Å	11.136(5)
c/Å	21.807(17)
α/°	90
β/°	94.17(5)
γ/°	90
Volume/$Å^3$	8529(10)
Z	8
ρ_{calc}/$g.cm^{-3}$	1.684
μ/mm^{-1}	15.63
F(000)	4328
Data range for refinement	8.0 – 1.20 Å
Index ranges	$-32 \leq h \leq 32$, $-10 \leq k \leq 9$, $-19 \leq l \leq 19$
Reflections collected	19501
Independent reflections	3333 [R_{int} = 0.075, R_{sigma} = 0.066]
Data/restraints/parameters	3333/402/552
Goodness-of-fit on F^2	1.029
Final R indexes [I>=2σ (I)]	R_1 = 0.061, wR_2 = 0.134
Final R indexes [all data]	R_1 = 0.080, wR_2 = 0.141
Largest diff. peak/hole / e $Å^{-3}$	0.42/-0.49

3. Powder X-ray diffraction patterns

The data were obtained from freshly prepared MOF samples that had been washed several times with MeOH. MOF crystals were analysed right after removing them from MeOH. The two-dimensional images of the Debye rings were integrated with 2DP to give 2θ vs I diffractograms. Predicted powder patterns were generated from single crystal structures using Mercury.

For aging experiments on the frameworks, after washing as-synthesized samples several times with MeOH, they were activated and were aged in air at 70-85% relative humidity at 20 °C.

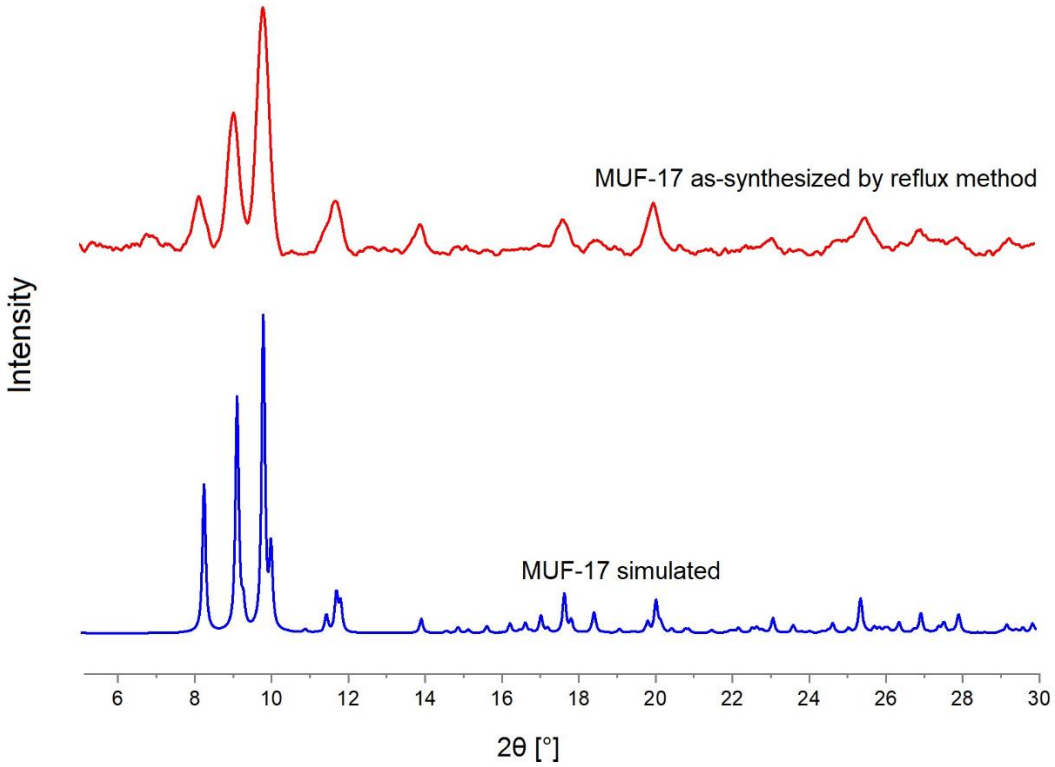

Figure S1. PXRD patterns of MUF-17 simulated from its SCXRD structure and as-synthesized MUF-17 prepared by the reflux method.

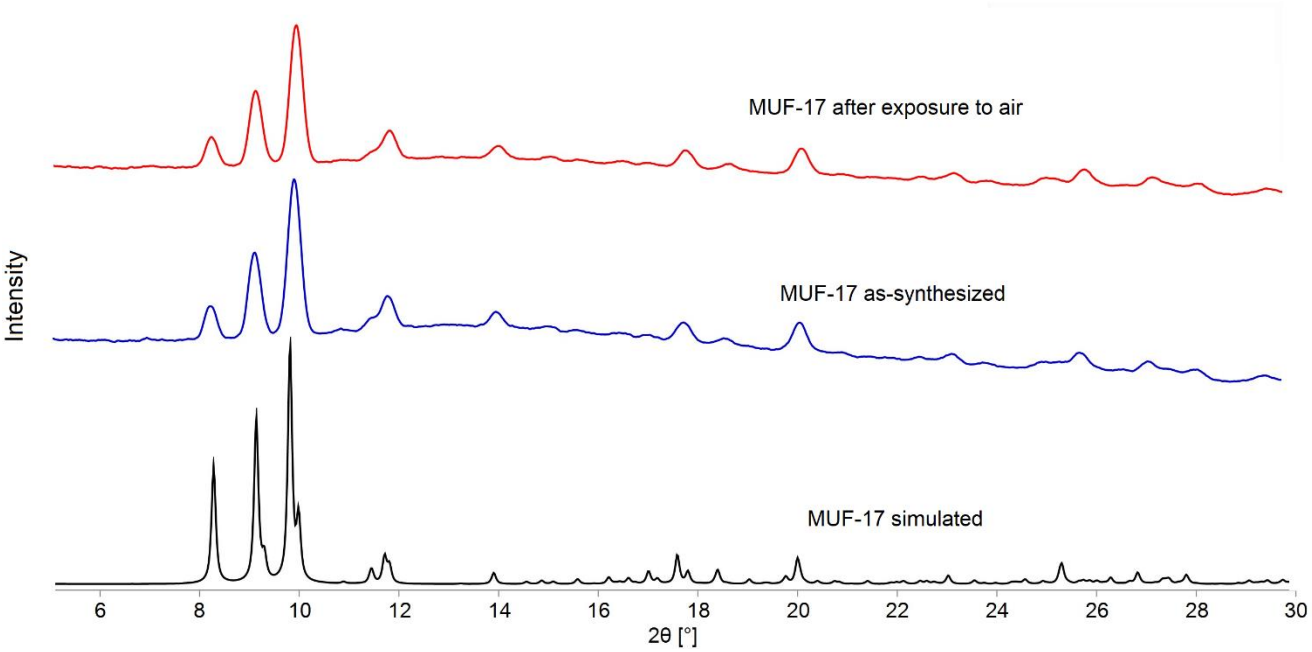

Figure S2. PXRD patterns of MUF-17 showing that its structure remains unchanged after exposure to air with relative humidity of >70% for at least 20 months.

4. Thermogravimetric analysis

Thermogravimetric analysis (TGA) was performed using a TA Instruments Q50 instrument. Measurements were made on approximately 5 mg of activated sample under a N_2 flow with a heating rate of 5 °C/min. Activated samples were kept at atmosphere after activation. Weight loss at low temperatures are attributed to the removal of water vapor trapped in the pores.

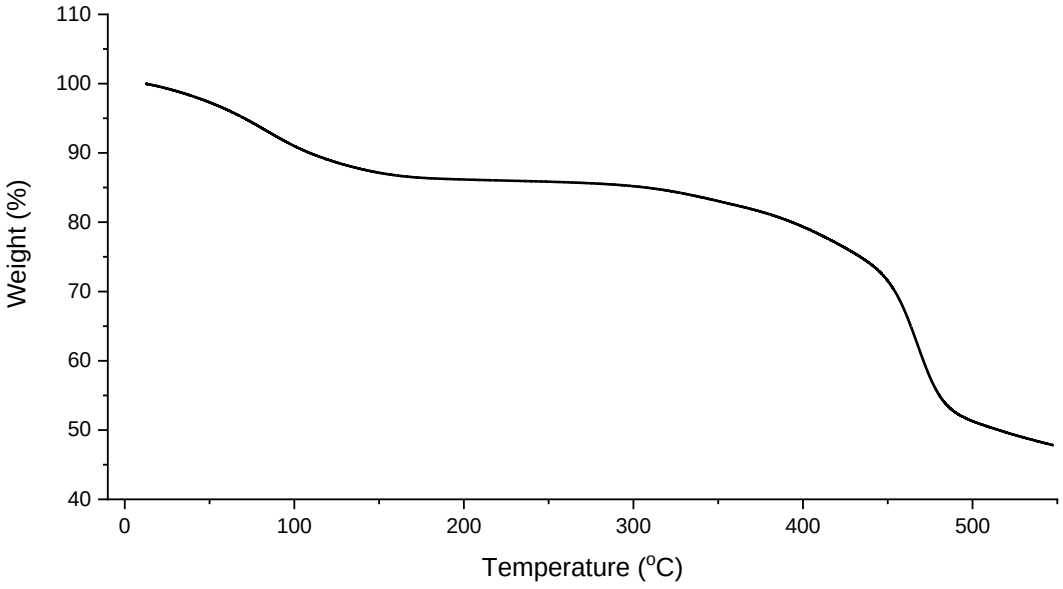

Figure S3. TGA curve of MUF-17.

5. Gas adsorption measurements

The adsorption isotherms were measured with a volumetric adsorption apparatus (Quantachrome-Autosorb-iQ2). Ultra-high purity gases were used as received from BOC Gases. The as-synthesized samples were washed with dry methanol several times and 100-200 mg was transferred into a pre-dried and weighed sample tube and heated at rate of 10°C/min to a temperature of 130 °C under a dynamic vacuum at 10^{-6} Torr then held for 20 hours. Accurate sample masses were calculated using degassed samples after the sample tube was backfilled with nitrogen.

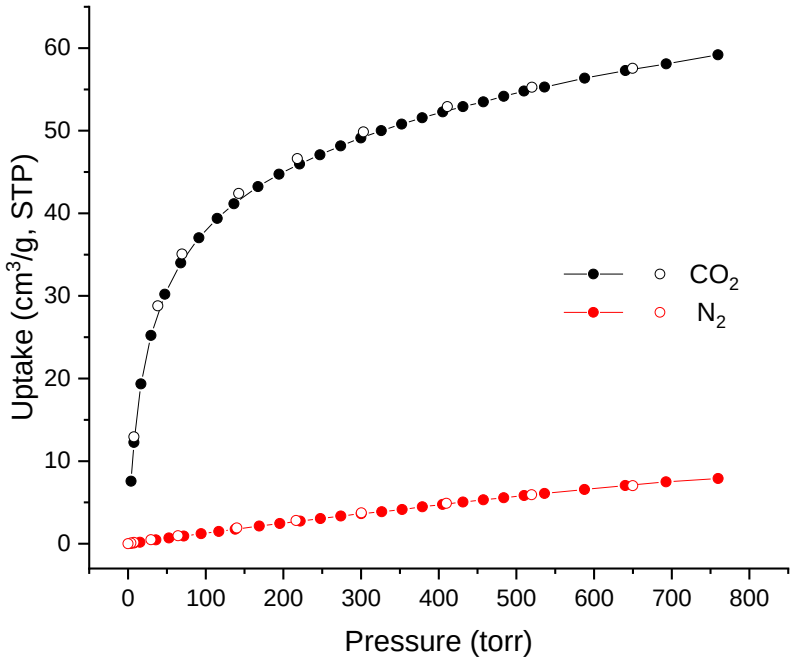

Figure S4. Experimental CO_2 and N_2 adsorption (solid symbols) and desorption (open symbols) isotherms of MUF-17 at 293 K.

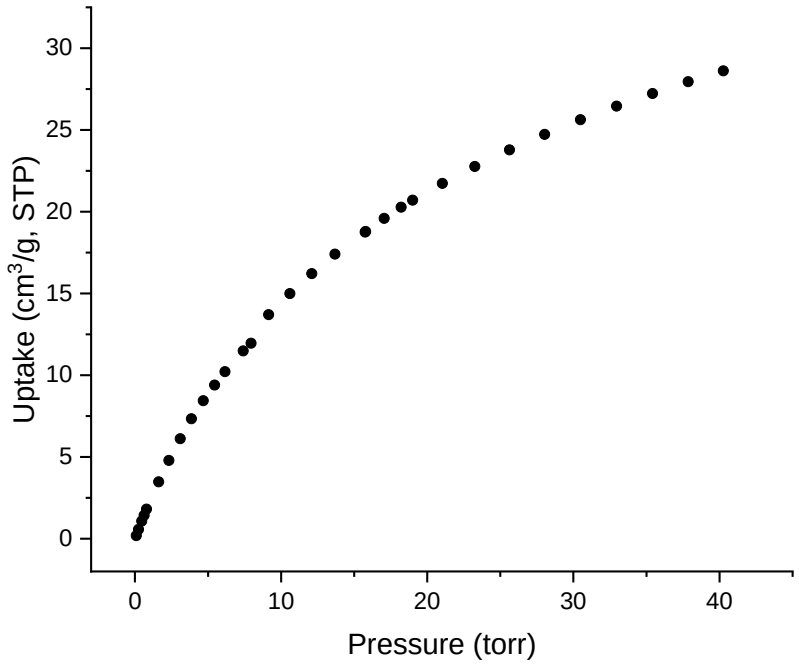

Figure S5. Experimental CO_2 isotherm of MUF-17 in the low pressure region at 293 K.

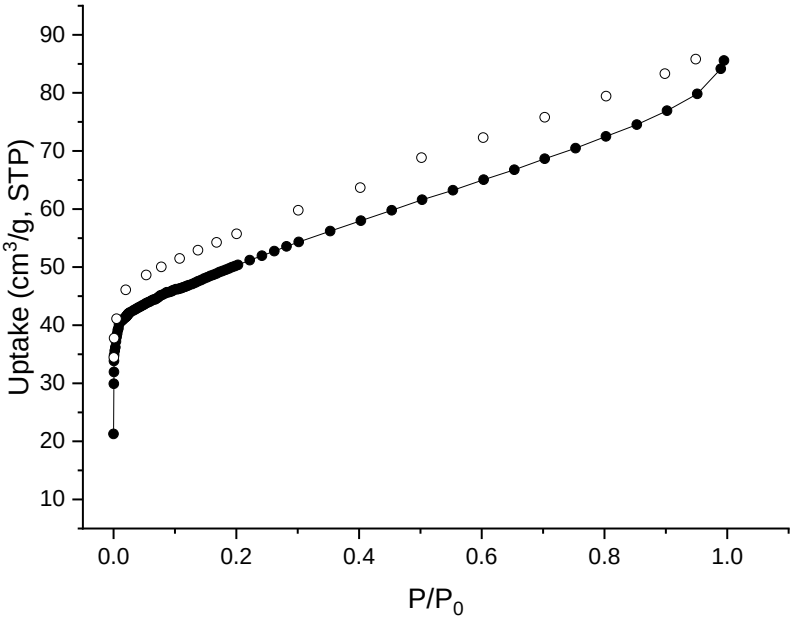

Figure S6. Volumetric adsorption (filled circles) and desorption (open circles) isotherms of N_2 measured at 77 K for MUF-17.

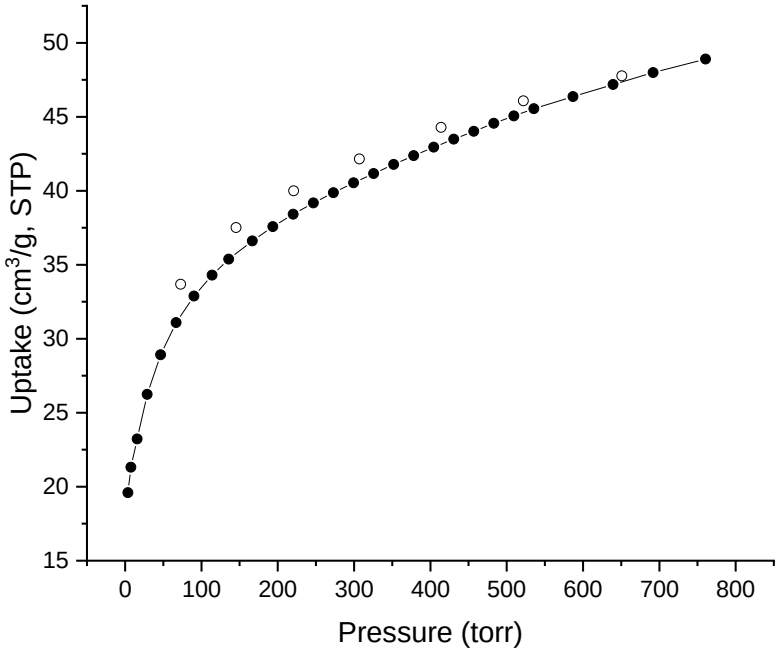

Figure S7. Volumetric adsorption (filled circles) and desorption (open circles) isotherms of C_3H_8 measured at 293 K for MUF-17.

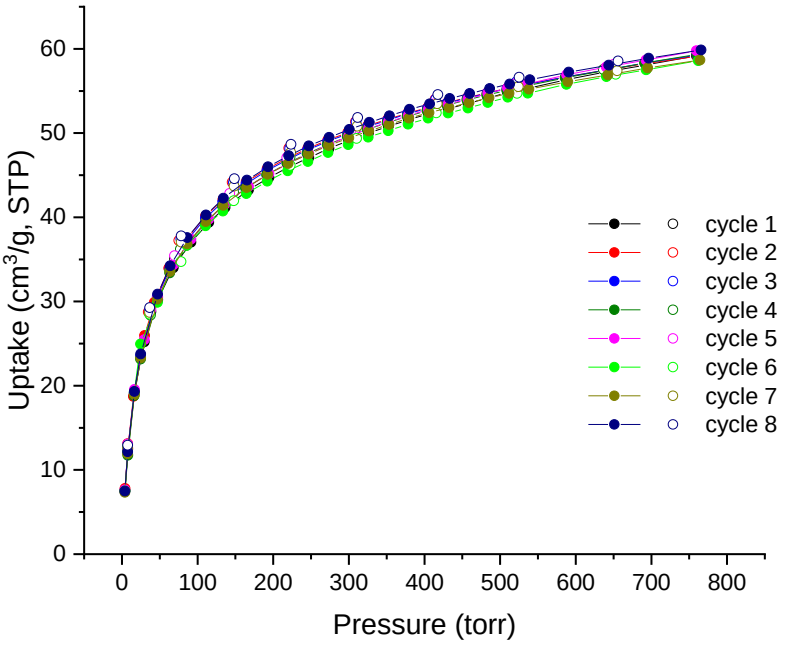

Figure S8. CO_2 isotherms of MUF-17 at 293 K measured on the same sample over multiple cycles.

6. Heat of adsorption

Isosteric heat of adsorption[2] (Q_{st}) values were calculated from isotherms measured at 283 K, 293, 298 K and 308 K for CO_2 and 273 K, 293K and 298K for N_2. The isotherms were first fit to a viral equation:

$$\ln P = \ln N + \frac{1}{T}\sum_{i=0}^{m} a_i N^i + \sum_{i=0}^{n} b_i N^i$$

Where N is the amount of gas adsorbed at the pressure P, a and b are virial coefficients, m and n are the number of coefficients required to adequately describe the isotherm. To calculate Q_{st}, the fitting parameters from the above equation were input in to the following equation:

$$Q_{st} = -R\sum_{i=0}^{m} a_i N^i$$

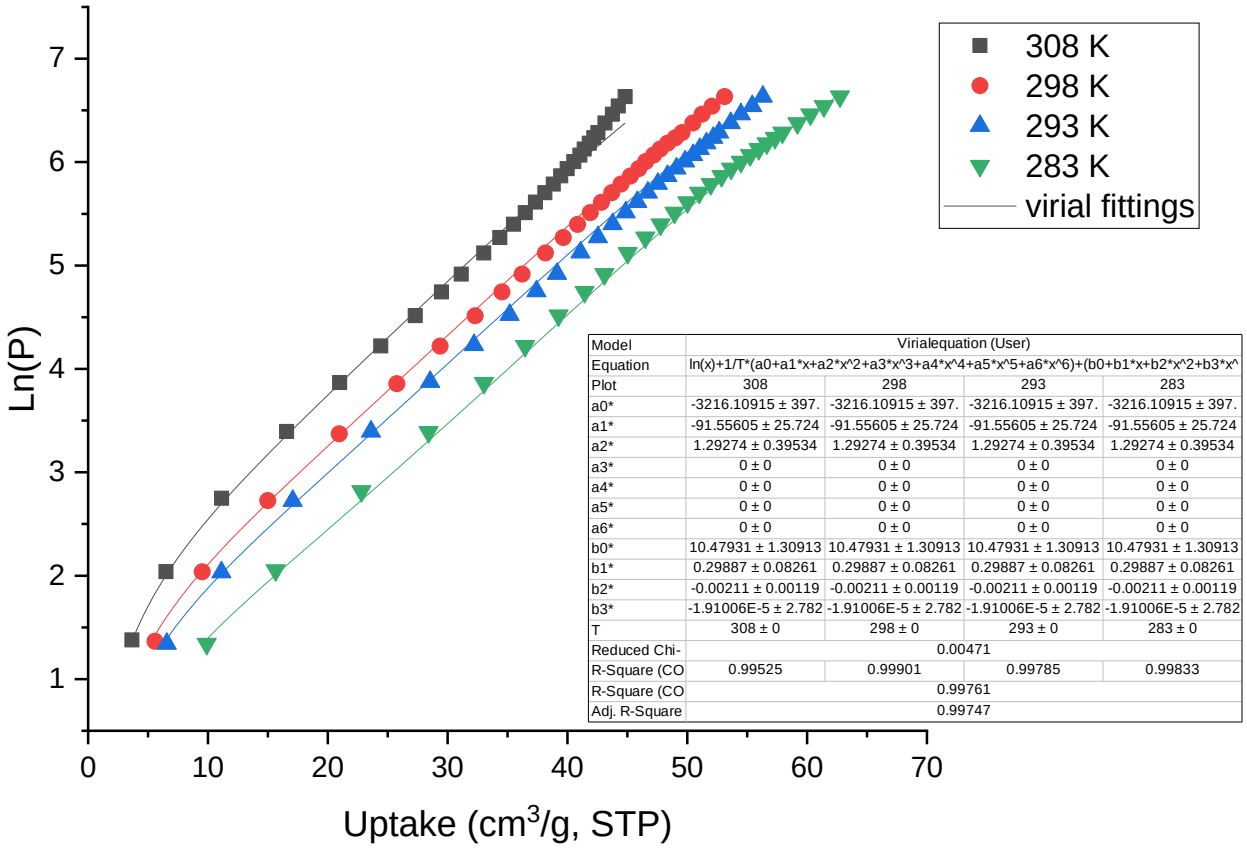

Model	Virialequation (User)			
Equation	ln(x)+1/T*(a0+a1*x+a2*x^2+a3*x^3+a4*x^4+a5*x^5+a6*x^6)+(b0+b1*x+b2*x^2+b3*x^			
Plot	308	298	293	283
a0*	-3216.10915 ± 397.	-3216.10915 ± 397.	-3216.10915 ± 397.	-3216.10915 ± 397.
a1*	-91.55605 ± 25.724	-91.55605 ± 25.724	-91.55605 ± 25.724	-91.55605 ± 25.724
a2*	1.29274 ± 0.39534	1.29274 ± 0.39534	1.29274 ± 0.39534	1.29274 ± 0.39534
a3*	0 ± 0	0 ± 0	0 ± 0	0 ± 0
a4*	0 ± 0	0 ± 0	0 ± 0	0 ± 0
a5*	0 ± 0	0 ± 0	0 ± 0	0 ± 0
a6*	0 ± 0	0 ± 0	0 ± 0	0 ± 0
b0*	10.47931 ± 1.30913	10.47931 ± 1.30913	10.47931 ± 1.30913	10.47931 ± 1.30913
b1*	0.29887 ± 0.08261	0.29887 ± 0.08261	0.29887 ± 0.08261	0.29887 ± 0.08261
b2*	-0.00211 ± 0.00119	-0.00211 ± 0.00119	-0.00211 ± 0.00119	-0.00211 ± 0.00119
b3*	-1.91006E-5 ± 2.782	-1.91006E-5 ± 2.782	-1.91006E-5 ± 2.782	-1.91006E-5 ± 2.782
T	308 ± 0	298 ± 0	293 ± 0	283 ± 0
Reduced Chi-	0.00471			
R-Square (CO	0.99525	0.99901	0.99785	0.99833
R-Square (CO	0.99761			
Adj. R-Square	0.99747			

Figure S9. Virial equation fits for CO_2 adsorption isotherms of MUF-17.

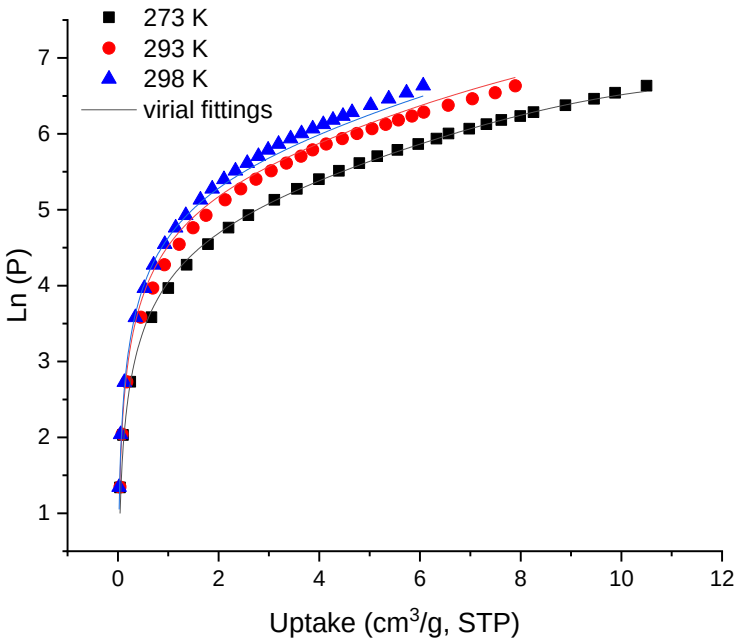

Model	Virial equation		
a0*	-1885.97998 ± 168.95246		
a1*	-22.47338 ± 40.74973	-22.47338 ± 40.74973	-22.47338 ± 40.74973
a2*	0 ± 0	0 ± 0	0 ± 0
a3*	0 ± 0	0 ± 0	0 ± 0
a4*	0 ± 0	0 ± 0	0 ± 0
a5*	0 ± 0	0 ± 0	0 ± 0
a6*	0 ± 0	0 ± 0	0 ± 0
b0*	11.04709 ± 0.58538	11.04709 ± 0.58538	11.04709 ± 0.58538
b1*	-0.03418 ± 0.14472	-0.03418 ± 0.14472	-0.03418 ± 0.14472
b2*	0.02535 ± 0.00798	0.02535 ± 0.00798	0.02535 ± 0.00798
b3*	-0.0013 ± 5.56895E-4	-0.0013 ± 5.56895E-4	-0.0013 ± 5.56895E-4
T	273 ± 0	293 ± 0	298 ± 0
Reduced Chi-Sqr*	0.01165		
R-Square (COD)	0.99644	0.99289	0.9928
R-Square (COD)*		0.99404	
Adj. R-Square*	0.99366		

Figure S10. Virial equation fits for N_2 adsorption isotherms of MUF-17.

7. IAST calculations

Mixed gas adsorption isotherms and gas selectivities for different mixtures of CO_2/N_2 at 273 K and 298 K were calculated based on the ideal adsorbed solution theory (IAST) proposed by Myers and Prausnitz[3]. In order to predict the adsorption performance of MUF-17 toward the separation of binary mixed gases, the single-component adsorption isotherms were first fit to a Dual Site Langmuir model, as below:

$$q = \frac{q_1 b_1 P}{1 + b_1 P} + \frac{q_2 b_2 P}{1 + b_2 P}$$

Where q is the uptake of a gas; P is the equilibrium pressure and q_1, b_1, t_1, q_2, b_2 and t_2 are constants. These parameters were used subsequently to carry out the IAST calculations.

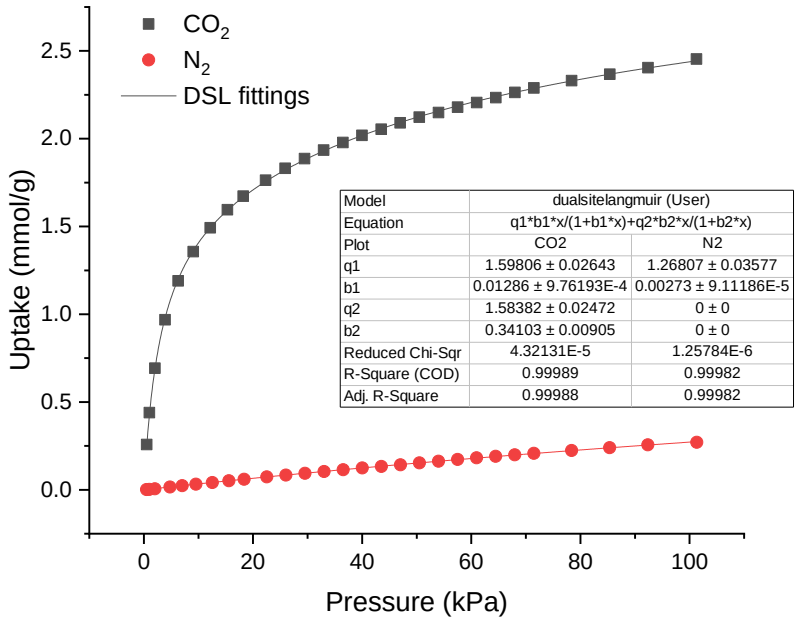

Model	dualsitelangmuir (User)	
Equation	q1*b1*x/(1+b1*x)+q2*b2*x/(1+b2*x)	
Plot	CO2	N2
q1	1.59806 ± 0.02643	1.26807 ± 0.03577
b1	0.01286 ± 9.76193E-4	0.00273 ± 9.11186E-5
q2	1.58382 ± 0.02472	0 ± 0
b2	0.34103 ± 0.00905	0 ± 0
Reduced Chi-Sqr	4.32131E-5	1.25784E-6
R-Square (COD)	0.99989	0.99982
Adj. R-Square	0.99988	0.99982

Figure S11. Dual-site Langmuir fits of the CO_2 and N_2 isotherms of MUF-17 at 298 K.

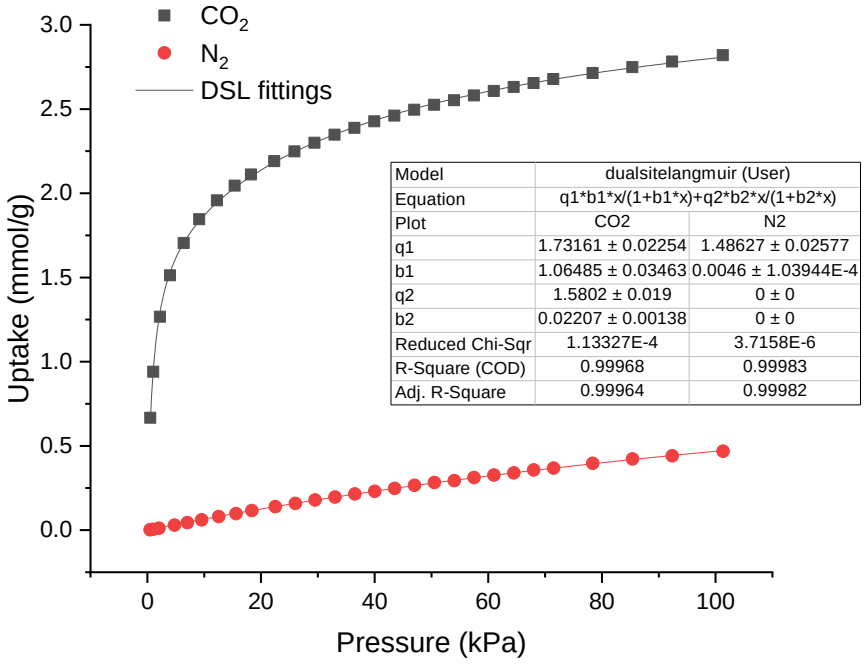

Model	dualsitelangmuir (User)	
Equation	q1*b1*x/(1+b1*x)+q2*b2*x/(1+b2*x)	
Plot	CO2	N2
q1	1.73161 ± 0.02254	1.48627 ± 0.02577
b1	1.06485 ± 0.03463	0.0046 ± 1.03944E-4
q2	1.5802 ± 0.019	0 ± 0
b2	0.02207 ± 0.00138	0 ± 0
Reduced Chi-Sqr	1.13327E-4	3.7158E-6
R-Square (COD)	0.99968	0.99983
Adj. R-Square	0.99964	0.99982

Figure S12. Dual-site Langmuir fits of CO_2 and N_2 isotherms of MUF-17 at 273 K.

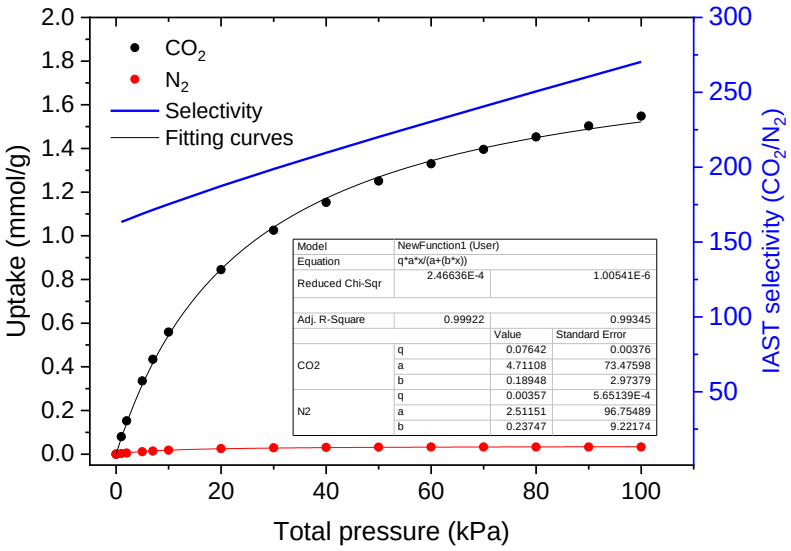

Figure S13. Mixed-gas isotherms and selectivity of MUF-17 predicted by IAST for a mixture of 15/85 CO_2/N_2 at 298 K.

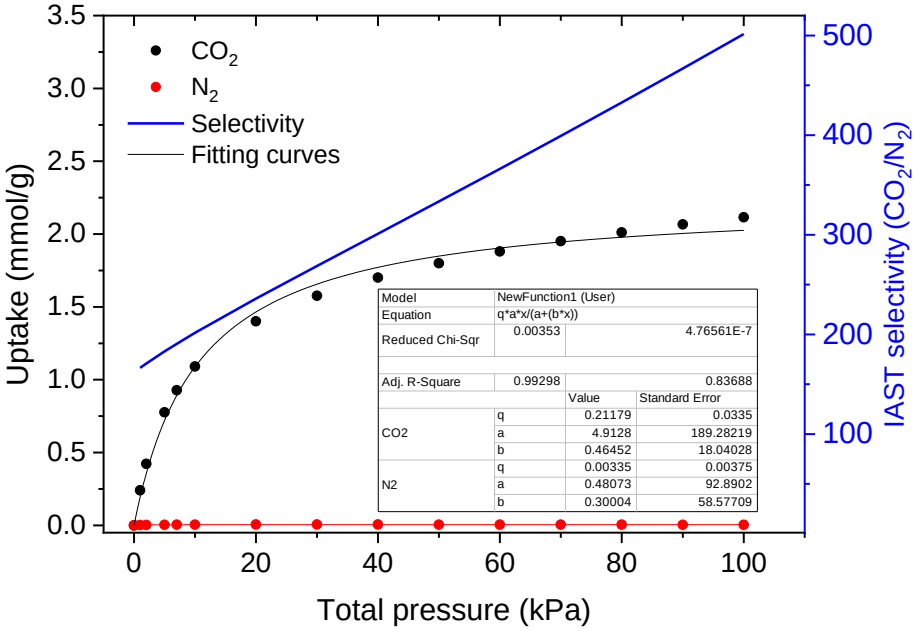

Figure S14. Mixed-gas isotherms and selectivity of MUF-17 predicted by IAST for a mixture of 50/50 CO_2/N_2 at 298 K.

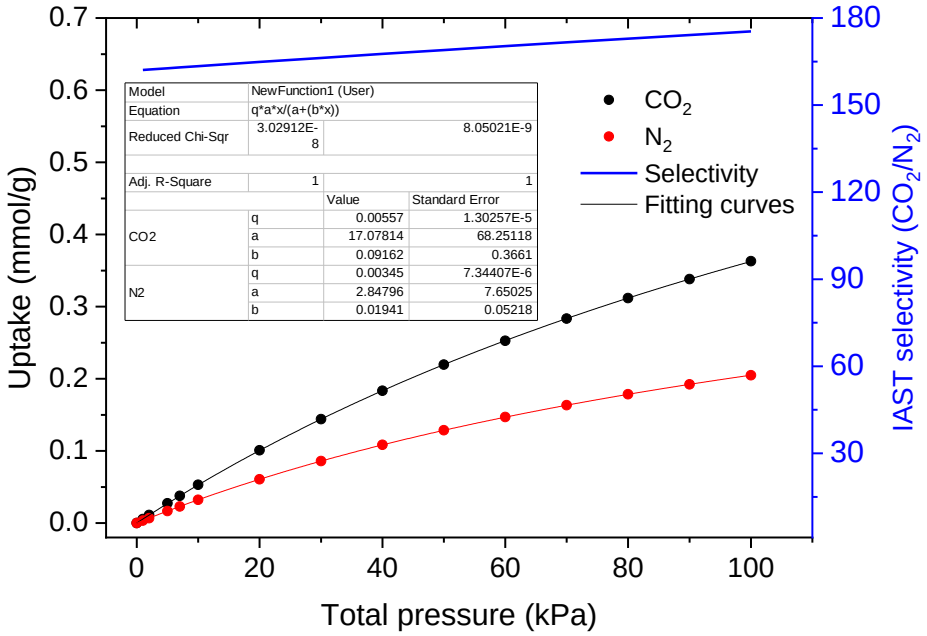

Figure S15. Mixed-gas isotherms and selectivity of MUF-17 predicted by IAST for a mixture of 1/99 CO_2/N_2 at 298 K.

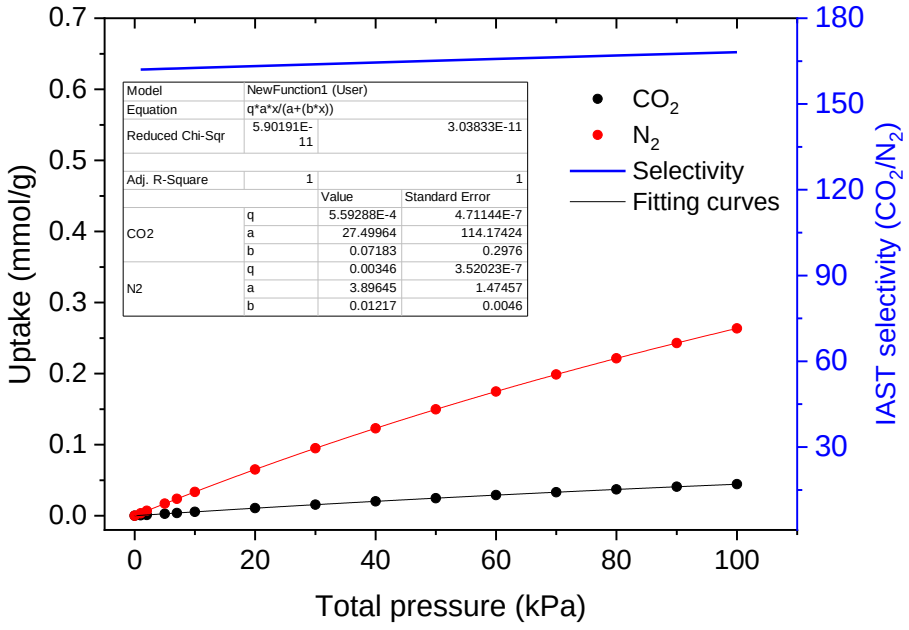

Figure S16. Mixed-gas isotherms and selectivity of MUF-17 predicted by IAST for a mixture of 0.1/99.9 CO_2/N_2 at 298 K.

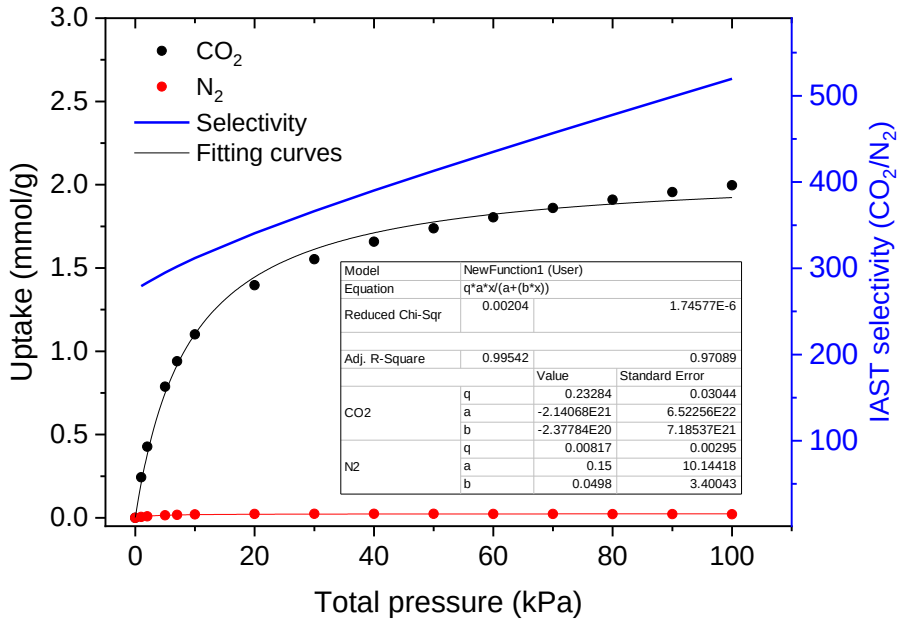

Figure S17. Mixed-gas isotherms and selectivity of MUF-17 predicted by IAST for a mixture of 15/85 CO_2/N_2 at 273 K.

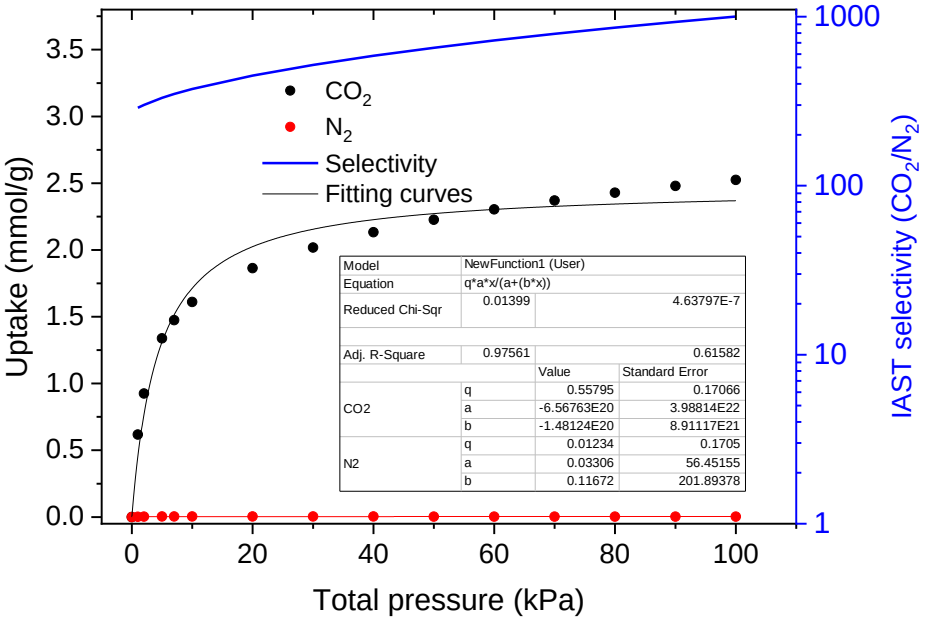

Figure S18. Mixed-gas isotherms and selectivity of MUF-17 predicted by IAST for a mixture of 50/50 CO_2/N_2 at 273 K.

8. Breakthrough separation experiment

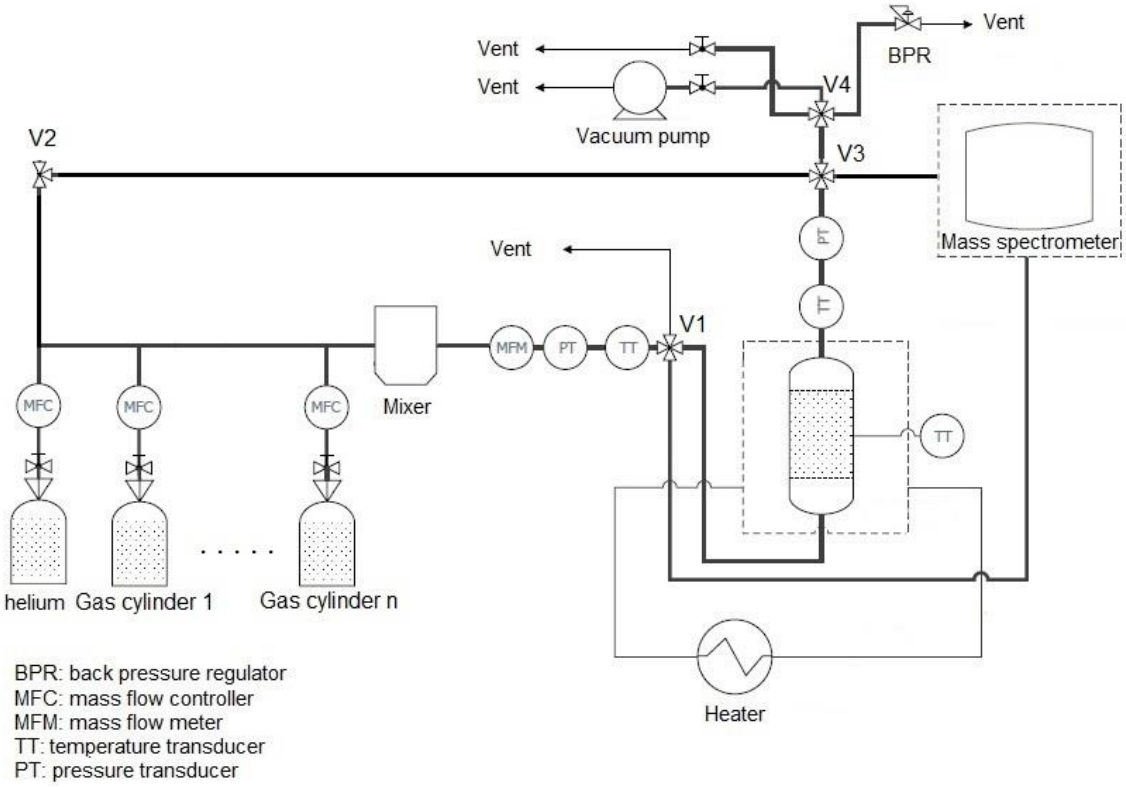

Figure S19. A schematic of the experimental column breakthrough setup.

Activated MUF-17 (0.95 g) was placed in an adsorption column (6.4 mm in diameter × 11 cm in length) to form a fixed bed. The adsorbent was activated at 130 °C under high vacuum for 7 hours and then the column was left under vacuum for another 3 hours while being cooled to 20 °C. The column was then purged under a 20 mL_N/min flow of He gas for 1 hr at 1.1 bar prior to the breakthrough experiment. A gas mixture containing CO_2/N_2 was introduced to the column at 1.1 bar (and 8 bar for high pressure experiment) and 25 °C. For the breakthrough in wet condition, water vapour was introduced by bubbling the gas stream through a temperature-controlled humidifier and the relative humidity determined by mass spectrometry.

A feed flowrate of 6 mL_N/min (10 mL_N/min for 1/99 CO_2/N_2 mixture) was set. The operating pressure was controlled at 1.1 or 8 bar with a back-pressure regulator. The outlet composition was continuously monitored by a SRS UGA200 mass spectrometer. The CO_2 was deemed to have broken through from the column when its concentration reached 600 ppmv.

Humid breakthrough experiment**:** The same flowrate and mixture composition to that of dry experiment was used for humid breakthrough measurement.

Adsorbent regeneration

The adsorbates (primarily CO_2) were stripped from the column to regenerate the adsorbent by purging with helium at 70 °C and a flow rate of 10 mL_N/min at 1.1 bar. For the recycling experiments, the adsorption bed was subsequently used to separate CO_2/N_2 15/85 (6 mL/min) before being regenerated again with a flow of helium at 70 °C. This process was repeated 30 times.

Alternatively, the adsorption bed could be regenerated under a dynamic vacuum (turbomolecular pump) for around 30-40 minutes at 70 °C, but this procedure was not typically employed.

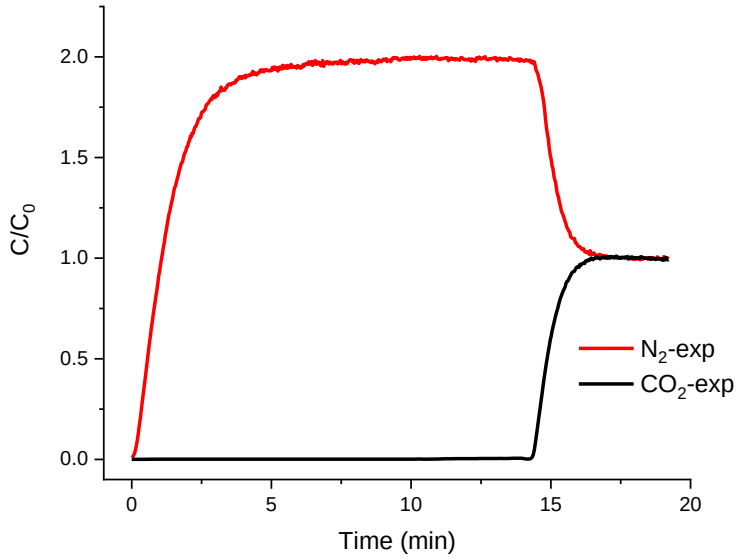

Figure S20. Experimental breakthrough curves for a mixture of CO_2/N_2 50/50 at 1.1 bar and 298 K in an adsorption column packed with MUF-17.

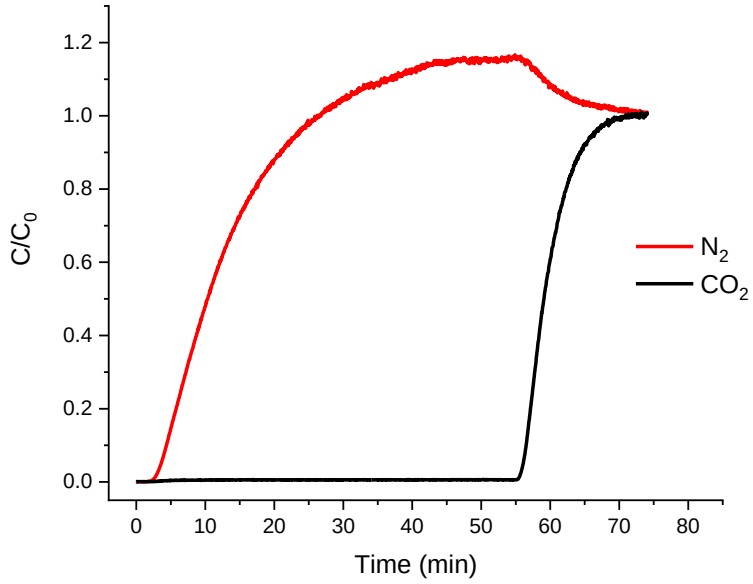

Figure S21. Breakthrough curves of CO_2/N_2 15/85 mixture at 298 K and 8 bar in an adsorption column packed with MUF-17.

9. Breakthrough curve simulations

9.1. Mathematical modelling

Considering a fixed bed adsorption column of length L filled with MUF-17, following assumptions were made to develop a mathematical model[4-6] that could be solved using proper numerical methods to calculate the concentration of gasses at different elapsed times along the bed.

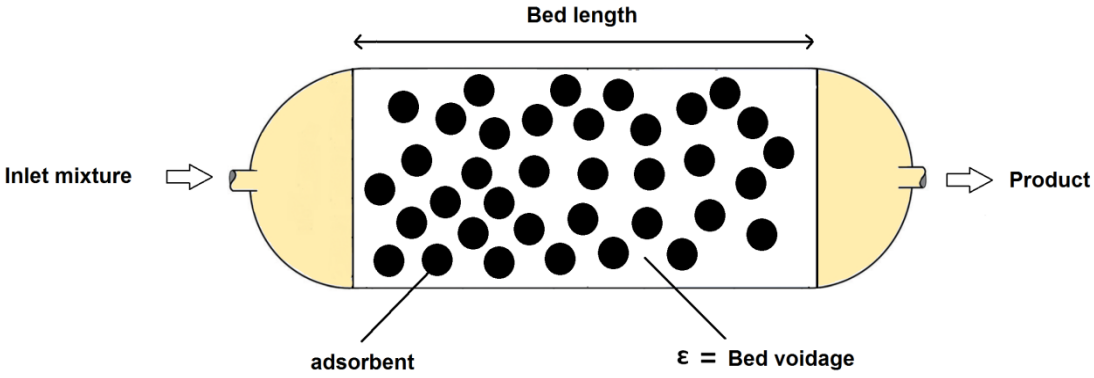

Figure S22. Schematic diagram of a fixed adsorption bed

The following assumptions were made:

- The dynamic behaviour of the fluid obeys an axial dispersion plug flow model in the bed.
- The gradient of the concentration along the radial and angular directions are neglected.
- The flow velocity is varied along the bed and it is calculated from the total mass balance equation.
- The gas property is described by the Peng-Robinson equation of state.
- Diffusion and adsorption into the particles is assumed as a lump kinetic transfer model.
- The mass transfer rate is represented by the linear driving force model.
- The pressure drop is considered along the bed using the Ergun equation.
- The adsorption columns operate under isothermal conditions.
- Mixed gas isotherms calculated by IAST method were fitted by single site Langmuir model and fitting parameters were used for breakthrough curves simulations.

Based on the preceding assumptions, the component and overall mass balances in the bulk phase of the adsorption column are written as follow:

$$\varepsilon \frac{\partial C_i}{\partial t} = -\frac{\partial (uC_i)}{\partial z} + \varepsilon D_{ax,i} \frac{\partial^2 C_i}{\partial z^2} - (1-\varepsilon)\rho_s \frac{\partial q_i}{\partial t}$$

$$\varepsilon \frac{\partial C}{\partial t} = -\frac{\partial (uC)}{\partial z} - (1-\varepsilon)\rho_s \sum_{1}^{n_c} (\frac{\partial q_i}{\partial t})$$

Where C_i and q_i are, respectively, concentration of components in the gas phase and in the adsorbed phase, z is the axial coordinate in the bed, D_{ax} is the effective axial dispersion coefficient, *u* is the superficial gas velocity, ρ_s is the adsorbent density, n_c is the number of the adsorbed components in the mixture and ε is the bed voidage. The value of D_{ax} was calculated through the following equation[7]:

$$\frac{\varepsilon D_{ax,i}}{D_{m,i}} = 20 + 0.5\, Sc_i\, Re$$

Where *Re* is the Reynolds number and Sc is the Schmidt number and $D_{m,i}$ is the molecular diffusivity of component *i* in the mixture which was calculated by following equation:

$$D_{m,i} = \frac{1-y_i}{\sum_{x=j}^{n} \frac{y_i}{D_{i,x}}}$$

Where y_i is the mole fraction of component I and $D_{i,x}$ is molecular diffusivity of component I in component x which was calculated by Wile-Lee equation[8]. Referring to the assumptions, the solid linear driving force (LDF) model is used to describe the mass transfer rate of the gas and solid phase[9]:

$$\frac{\partial q_i}{\partial t} = k_i (q_i^* - q_i)$$

Where k_i is the overall mass transfer coefficient, and a lumped parameter considering three different mass transfer resistances associated with film, macropore and micropore zone. As the overall mass transfer coefficient is in proportion to the steepness of breakthrough curves, the accurate value of it was obtained empirically by tuning its value until the steepness of the predicted and experimental breakthrough curves were the same. This mass transfer coefficient tuned in this way was later used to predict breakthrough curves for other feed mixtures and operating pressures. q_i^* is the equilibrium concentration of *i*th component in the adsorbed phase and is related to the concentration in the gas phase through isotherms. The IAST method was used to predict mixed gas isotherms and they were fitted by a Dual-Site Langmuir model. The pressure drop is defined by Ergun's equation as[10]:

$$\frac{\partial P}{\partial z} = -\left(\frac{37.5\,(1-\varepsilon)^2 \mu u}{\left(r_p \varphi\right)^2 \varepsilon^3} + 0.875\rho\, \frac{(1-\varepsilon)u^2}{r_p \varphi \varepsilon^3} \right)$$

Where P is the local pressure at the z axial coordinate, μ is the gas viscosity, φ is the shape factor and ρ is the gas density. Identical conditions to the experimental breakthrough measurement, including operating pressure, feed flowrate, temperature, bed size and amount of MOF, were used as input for simulations. All the parameters used for the simulations are tabulated in Table S2.

Table S2. Adsorption column parameters and feed characterizations used for the simulations for MUF-17.

Adsorption bed	***Dual-Site Langmuir fitting***
Length: 110 mm Diameter: 6.4 mm Amount of adsorbent in the bed: 0.95 g Bed voidage: 0.5 Adsorbent average radius: 0.05 mm k_{CO2}: 4.2 s^{-1} k_{N2}: 5.1 s^{-1}	Figures above ***Feed*** Total flow rate: 6 mL_N/min for 15/85 and 50/50 mixture and 10 for 1/99 and 0.1/99.9 mixture Temperature: 298 K Pressure: 1.1 bar

9.2. Numerical methods

Numerical solutions of the nonlinear parabolic PDEs derived from mass and momentum balance were conducted by an implicit method of lines using finite difference method for the spatial derivatives. Firstly, the second and first space derivatives were discreted by central and upwind- differential scheme (backward), respectively. In this way, the sets of partial equations were transformed to the sets of ODEs with respect to the time derivative terms. The length of the bed was divided into 50 increments and the set of equations were solved by the Implicit Euler method with a time step of one second.[11]

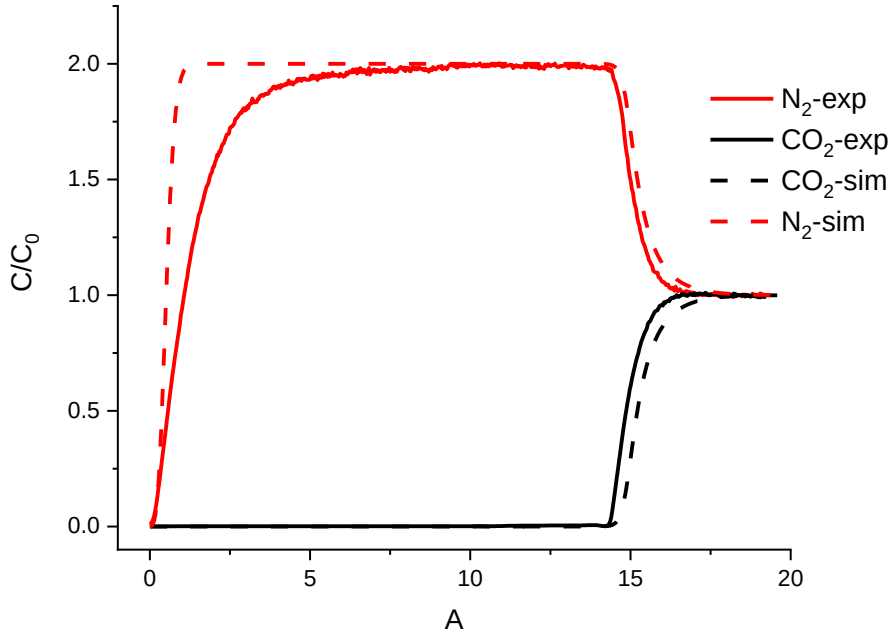

Figure S23. Predicted breakthrough curves for a mixture of 50/50 of CO_2/N_2 at 298 K and 1.1 bar compared with experimental breakthrough curves after tuning of the mass transfer coefficients (k_{CO2}: 4.2 s^{-1}, k_{N2}: 5.1 s^{-1}).

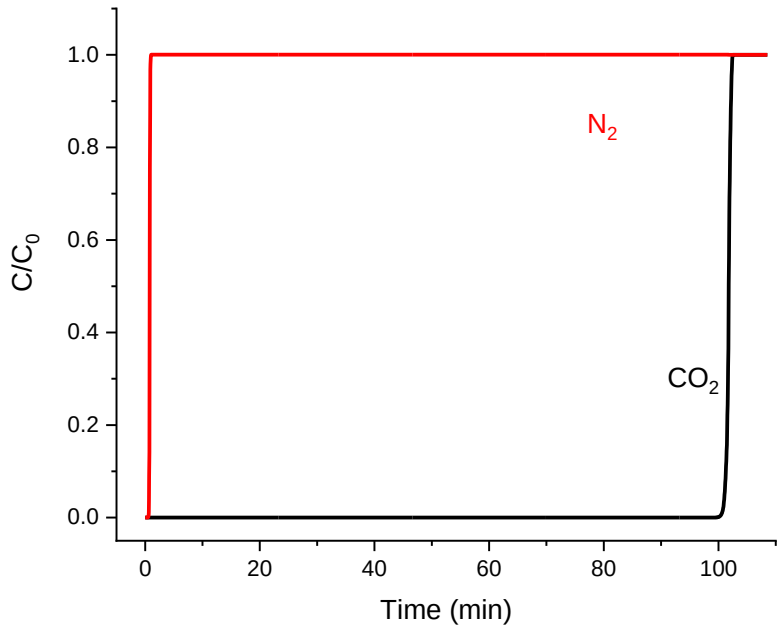

Figure S24. Simulated breakthrough curves for a 0.1/99.9 mixture of CO_2/N_2 at 1.1 bar and 298 K in an adsorption column packed with MUF-17.

10. Pelletization

MOF pellets were fabricated based on the following procedure:

i. MUF-17 (~1 g) was gently ground using mortar and pestle.
ii. The ground sample was transferred to a 20 mL vial and 1 mL of DMF was added. A viscous suspension was obtained after sonicating for half an hour. The suspension was stirred for another 30 mins.
iii. PVDF powder (50 mg) was gradually added over the course of 1 hour and the mixture was stirred overnight to make a viscous paste.
iv. The paste was transferred into a plastic syringe and squeezed it out into a thin noodle on a glass slide.
v. The noodle was cut into small pellets and dried under vacuum at 140 °C for 6 hours.

11. References

1. Qazvini, O. T.; Babarao, R.; Telfer, S. G., Multipurpose Metal–Organic Framework for the Adsorption of Acetylene: Ethylene Purification and Carbon Dioxide Removal. *Chem. Mater.* **2019,** *31* (13), 4919-4926.
2. Dincă, M.; Dailly, A.; Liu, Y.; Brown, C. M.; Neumann, D. A.; Long, J. R., Hydrogen Storage in a Microporous Metal−Organic Framework with Exposed Mn2+ Coordination Sites. *J. Am. Chem. Soc.* **2006,** *128* (51), 16876-16883.
3. Myers, A.; Prausnitz, J. M., Thermodynamics of mixed-gas adsorption. *AIChE J.* **1965,** *11* (1), 121-127.
4. Qazvini, O. T.; Fatemi, S., Modeling and simulation pressure–temperature swing adsorption process to remove mercaptan from humid natural gas; a commercial case study. *Sep. Purif. Technol.* **2015,** *139*, 88-103.
5. Mehdipour, M.; Fatemi, S., Modeling of a PSA-TSA Process for Separation of CH4from C2Products of OCM Reaction. *Sep. Sci. Technol.* **2012,** *47* (8), 1199-1212.
6. Chahbani, M. H.; Tondeur, D., Mass transfer kinetics in pressure swing adsorption. *Sep. Purif. Technol.* **2000,** *20* (2), 185-196.
7. Bird, R. B., Transport phenomena. *Applied Mechanics Reviews* **2002,** *55* (1), R1-R4.
8. Perry, R.; Green, D.; Maloney, J., *Chemical engineers handbook*. 8th edition ed.; The McGraw Hill Companies, Inc: 2008.
9. Farooq, S.; Ruthven, D. M., A comparison of linear driving force and pore diffusion models for a pressure swing adsorption bulk separation process. *Chem. Eng. Sci.* **1990,** *45* (1), 107-115.
10. Yang, R. T., *Gas separation by adsorption processes*. Butterworth-Heinemann: 2013.
11. Kiusalaas, J., *Numerical methods in engineering with Python 3*. Cambridge university press: 2013.